Sensors & Actuators: A. Physical 346 (2022) 113882

Contents lists available at ScienceDirect

Sensors and Actuators: A. Physical

journal homepage: www.journals.elsevier.com/sensors-and-actuators-a-physical

Effect of graphene on the piezoelectric properties of cement-based piezoelectric composites

Huang Hsing Pan [a,*], Ting-Zu Lai [a], Arnon Chaipanich [b,c], Thanyapon Wittinanon [b]

[a] Department of Civil Engineering, National Kaohsiung University of Science and Technology, Kaohsiung 80778, Taiwan
[b] Department of Physics and Materials Science, Faculty of Science, Chiang Mai University, Chiang Mai 50200, Thailand
[c] Center of Excellence in Materials Science and Technology, Materials Science Research Center, Faculty of Science, Chiang Mai University, Chiang Mai 50200, Thailand

ARTICLE INFO

Keywords:
Graphene
Piezoelectric cementitious composites
Piezoelectricity
Sensing
Structural health monitoring

ABSTRACT

Two types of graphene, namely, graphene oxide (GO) and multilayer graphene nanoplatelets (GNPs), were added to a 0–3-type cement-based piezoelectric composite to investigate the piezoelectric properties of the composite. The aforementioned composite contained a cement matrix and lead zirconate titanate inclusions, each of which accounted for 50% of the composite volume. The results obtained by using ultrasonic vibrations and a hydrometer indicated that the optimal dispersion times of GO in pure water and GNPs in ethanol were 30 and 15 min, respectively. The addition of GO to the aforementioned composite decreased the composite's relative permittivity (ε_r) and increased dielectric loss and electrical resistance, resulting in difficulties in poling and poor polarization efficiency. GO is not conducive to improving the piezoelectric properties (piezoelectric charge coefficient d_{33}, piezoelectric voltage coefficient g_{33}, ε_r, and electromechanical coupling coefficient k_t) of piezoelectric composites. GNP addition to cement can reduce the resistivity and increase dielectric loss of cement composites. The composites with a lower resistance can be polarized easily. The appropriate addition of GNPs can improve the polarization efficiency, thereby enhancing the piezoelectric properties of cementitious composites. In this study, the optimal addition of GNPs was 0.3%. Wet-mixing of GNP-containing cementitious composites with a superplasticizer in ethanol can further improve the piezoelectric properties of this composite (d_{33} = 123 pC/N, g_{33} = 22.6 $\times 10^{-3}$ V·m/N, ε_r = 615, and k_t = 20.2%). The GNP-containing cementitious composite mixed with a superplasticizer exhibited a high k_t; thus, this composite has potential for use as a green energy material.

1. Introduction

Similar to the multiphase microstructure of iron, the hydration composition of cement is diverse and complex, which allows the development of unique cement-based materials (cementitious materials) for use in civil infrastructure. Cementitious materials have advantageous physical, mechanical, electrical, and thermal properties; therefore, they are used to produce many useful materials and devices, such as floating concrete [1,2], ultrahigh-performance concrete [3–5], piezoresistive-based self-sensing concrete [6–9], self-healing concrete [10–12], and cement-based piezoelectric sensors and actuators [13–16]. The use of lightweight aggregates, pozzolanic materials, biomimetic materials, and additives in a cement matrix is common for developing cementitious materials with unique properties.

In the past decade, many researchers have used graphene as an additive to enhance the mechanical properties and durability of cementitious materials [17–29]. Compared with few-layer and single-layer graphene, graphene oxide (GO) and multilayer graphene nanoplatelets (GNPs) are more commonly used in cementitious materials because they are not expensive and easier to produce. GNPs have higher thermal and electrical conductivities than does GO; however, GNPs have a large specific surface area and exhibit strong van der Waals forces. Thus, poor mixing effects are achieved when GNPs are combined with cement. Therefore, GNPs must be uniformly dispersed in the cement matrix of cementitious materials (concrete and mortar) [30]. Furthermore, GO is more hydrophilic and more easily exfoliated in water (resulting in stable dispersions) than are GNPs; thus, GO is more commonly used than GNPs to improve the mechanical properties and durability of cementitious materials [17–20,23–29]. GO can promote the hydration kinetics of cement, stimulate the growth of hydration

* Corresponding author.
E-mail address: pam@nkust.edu.tw (H.H. Pan).

https://doi.org/10.1016/j.sna.2022.113882
Received 20 June 2022; Received in revised form 21 August 2022; Accepted 11 September 2022
Available online 15 September 2022

products, and form strong covalent bonds with hydration products [17]. The mixing of a favorable amount of GO in the cement matrix can effectively improve the mechanical properties, microstructure [19,20,23–25], durability [26], impermeability, corrosion resistance [29], and rheological behavior [31] of the cement matrix.

Because oxygen atoms can cause structural defects in GO, GO might not be a suitable additive for enhancing the thermal and electrical conductivities of cementitious materials [30]. Liu et al. [32] found that the electrical resistance of GO-containing mortars on oven-dried specimens was not considerably different from that of GO-free mortar, indicating that the addition of GO had little effect on the piezoresistive properties of the mortars. The piezoresistive effect refers to a change in the electrical resistance of a material when the material is loaded. The electrical resistance of mortar decreases with an increase in its GNP content; thus, with an increase in the GNP content, mortars transform from being insulators to conductors (refer to Fig. 7 in [32]). This implies that the addition of GNPs can improve the piezoresistive sensitivity of cementitious materials. If the agglomeration phenomenon of GNPs can be overcome, they will be superior to GO in improving the mechanical, electrical, and thermal properties of cementitious materials at an appropriate amount [21,22,25,30,32]. Several dispersion techniques for graphene materials, such as GO and GNPs, have been proposed in experimental studies [30,33–37]. For instance, graphene can be effectively dispersed using water-reducing admixtures (such as superplasticizers) and ultrasonic waves (mechanical vibration) (relevant results are presented in Table 2 of [30]). To achieve superior dispersion of GNP sheets, water-reducing admixtures are typically used in conjunction with ultrasonic vibrations [36,37]. Ultrasonic treatment can be applied to overcome the van der Waals interactions between the graphene sheets, making the dispersion of graphene in a solution easier.

Because of its unique electromechanical characteristics, graphene has been used to enhance the piezoresistive sensitivity of cementitious materials for structural health monitoring (SHM). GO has been used as a functional filler in only a few piezoresistive self-sensing cementitious materials. For example, a GO-containing cement paste with piezoresistive sensitivity under cyclic uniaxial compressive loads was investigated in a previous study [38]. Most researchers have focused on the use of reduced graphene oxide (rGO) and GNPs to investigate piezoresistive self-sensing materials. For instance, rGO, a graphene derivative obtained by removing oxygen functional groups from GO, has been used in piezoresistive pressure sensors [39], piezoelectric geopolymer composites [40], and piezoresistive mortar-containing multiwall carbon nanotubes (CNTs) [41]. GNPs can reduce the electrical resistivity of cementitious materials [21,30] and modify the microstructure and piezoresistive properties of cement-based composites [32,42]. The piezoresistive stability of self-sensing cementitious materials containing GNPs has been investigated under cyclic loading [43,44], tension and compression [45], and impact loads [46].

Cement-based piezoelectric composites (piezoelectric cementitious composites), with cement as the matrix and piezoelectric materials as functional inclusions, can be used as sensing elements for SHM. Lead zirconate titanate (PZT) and barium zirconate titanate are commonly selected as functional inclusions in the aforementioned composites. Cement-based piezoelectric composites have been developed in order to achieve acoustic matching with concrete materials for better sensing in structural health monitoring application in concrete structures. At 50% PZT ceramic volume content, the acoustic impedance is similar to that of concrete (≈9–10 × 10^6 kg/m^2·s). Piezoelectric cementitious composites exhibit piezoelectric properties if complete electric field polarization can be achieved. Because of their piezoelectric properties, piezoelectric cementitious composites can be used as sensing elements in piezoelectric sensors and actuators used in SHM for concrete structures and traffic monitoring [16,47–49]. Piezoelectric sensors with higher values for piezoelectric properties, such as piezoelectric charge coefficient (d_{33}) and piezoelectric voltage coefficient (g_{33}), have higher monitoring sensitivity in real-time SHM. Research on improving the piezoelectric properties of piezoelectric cementitious composites (as piezoelectric sensing elements) has been ongoing since 2001 [13–15,50–57].

The piezoelectric properties of 0–3-type cement-based piezoelectric composites (whose functional particles are randomly oriented in the cement matrix) can be enhanced by optimizing the manufacturing process, polarization conditions, and additives. For instance, in a previous study, the d_{33} value of a piezoelectric cementitious composite containing 50% PZT increased considerably from 55 pC/N to 106 pC/N when the composite was treated at 150 °C before and after electrode fabrication [15]. Thus, cement-based piezoelectric composites (as sensors and actuators) are used in the SHM of concrete structures, including the monitoring of strength development [16] and stress–strain behavior [49]. If the composite has an appropriate water-to-cement (w/c) ratio during mixing (e.g., $w/c = 10\%$), its d_{33} value can be further increased to 133 pC/N [57]. During the polarization process, a higher poling voltage and poling temperature [52–54] and an appropriate poling time [55] are typically used to obtain cement-based piezoelectric composites with higher d_{33} and relative permittivity (ε_r) values. Moreover, the use of pozzolanic materials, such as silica fume [58,59], slag, and fly ash [60], as admixtures in cementitious composites can enhance the piezoelectricity of these composites. Materials such as carbon [61], carbon black [62,63], nano-quartz powders [64], CNTs [65], and kaolin [66] have also been used as additives to improve the piezoelectric properties of cementitious composites.

Since 2014, graphene has attracted increasing attention as a material for improving the piezoelectricity of cementitious materials and geopolymer composites. Chang et al. [67] indicated that some highly ordered compounds of GO (such as clamped and unzipped GO) exhibit piezoelectric responses and that a higher oxygen concentration causes an increase and decrease in the d_{33} values of the clamped GO and unzipped GO, respectively. Candamano et al. [68] found that geopolymer mortar with 1% GNPs exhibits a d_{33} value of 11.99 pC/N within a pressure range of 0–2500 N. Certain geopolymer materials, such as metakaolin-containing GNPs, exhibit a piezoelectric effect under cyclic compression but not under completely dry conditions [69]. Although the piezoelectric performance of graphene is considerably worse than that of piezoelectric ceramics such as PZT, graphene can be regarded as a piezoelectric material to a certain extent. Jaitanong et al. [70] investigated a cementitious composite consisting of silica/cement as a binder, lead niobate zirconate titanate as functional particles, and 0–5% GNPs as an additive and found that the ε_r value and dielectric loss of this

Table 1
Properties of PZT ceramic material*.

Parameter	Properties
Piezoelectric charge coefficient d_{33} (× 10^{-12}C/N)	470
Piezoelectric voltage coefficient g_{33} (× 10^{-3}V-m/N)	24
Relative permittivity ε_r ($=\varepsilon_{33}^T/\varepsilon_0$)	2100
Thickness electromechanical coupling coefficient k_t	0.72
Density ρ (× 10^3kg/m^3)	7.9
Dielectric loss D	0.015

* Provided by Eleceram Technology Co., Ltd. (Taiwan)

Table 2
Properties of GO and GNPs.

	GO	GNPs
Diameter (μm)	0.5–5	0.5–20
Thickness (nm)	0.8–1.2	1–10
Specific surface area (m^2/g)	*	50–70
TAP density (g/cm^3)	0.981	0.075
Appearance	Black	Black
C (%)	51.35	*
O (%)	40.78	*
Electrical conductivity (S/cm)	*	70000

* Note: The information is not provided in the product reports.

composite increased with an increasing GNP content. However, they could not identify the specific GNP contents that resulted in an enhanced dielectric effect. Studies on the piezoelectric properties of graphene-containing cementitious composites are limited. When the piezoelectric properties of graphene-containing cementitious materials are studied, the optimal graphene content and agglomeration properties should be determined.

In this study, the piezoelectric properties of a 0–3-type PZT/cement composite were investigated after the addition of GO and GNPs. The composite contained a cement matrix and PZT inclusions. First, the optimal dispersion time of graphene was determined by using ultrasonic vibration to reduce graphene agglomeration. Subsequently, graphene was added to the aforementioned cementitious composite. After polarization, the cementitious composite exhibited piezoelectricity; thus, the polarized composite was called piezoelectric cement (PEC). The optimal graphene content of the PEC was determined based on the maximum values of d_{33} and ε_r. The piezoelectric properties of the PEC containing the optimal graphene content were then examined under different graphene-mixing conditions.

2. Experiments

2.1. Materials

The investigated cementitious material was a 0–3-type PZT/cement composite, in which the cement matrix and PZT inclusions had a volume fraction of 50% each. The acoustic impedance of this composite is close to that of concrete [13], and it has been used as a PEC sensor for the SHM of concrete [16,49]. The matrix of this composite was fresh ASTM type I cement with a specific gravity and fineness of 3.16 and 321 m^2/kg, respectively. The inclusions were Ka-type unpolarized PZT ceramic materials (Eleceram Technology Co., Taiwan). The properties of PZT are presented in Table 1 (specific gravity = 7.9, d_{33} = 470 pC/N, ε_r = 2100, g_{33} = 24 mV·m/N, and dielectric loss D = 0.015). PZT particles with sizes in the range of 75–150 μm were used in the composite.

Two types of graphene, namely, GO and GNPs (Conjutek Co., Taiwan), were used as additives in the PEC. The scanning electron microscopy (SEM) images of GO and GNPs are shown in Fig. 1. The layered structure is the same as graphite crystal. The properties of graphene are listed in Table 2. The diameter and thickness of GO are 0.5–5 μm and 0.8–1.2 nm, respectively. GO is highly hydrophilic and easily dispersed in water. GNPs are a form of multilayer graphene that exhibit a diameter of 0.5–20 μm and a thickness of 1–10 nm. GNPs have a high electrical conductivity of 70,000 S/cm and are often used to reduce the electrical resistance of the materials. The specific surface area of GNPs is 50–70 m^2/g, and the particles agglomerate easily.

2.2. Dispersion of graphene

To reduce graphene agglomeration in PEC, graphene must be dispersed in a solution before mixing. Studies [34,71,72] have indicated that GO can be easily and uniformly dispersed in aqueous solvents. Moreover, GO agglomeration occurs even at a high GO content because of the van der Waals forces between its interfacial layers [23]. Therefore, pure water was selected as the solvent for GO dispersion in this study, and 100 mg of GO was added to 100 mL of pure water to form a 1-mg/mL GO solution. Water-based fluids, glycol-based fluids, and oils can act as solvents for dispersing GNPs [25,30,36,37]. After pilot experiments involving the dispersion of GNPs in different solvents were conducted, the GNPs agglomerated more easily in water than in ethanol. Moreover, the GNPs mixed with oils were found to be unsuitable for mixing with cementitious materials. Therefore, ethanol (specific gravity = 0.789) was selected as the solvent for the dispersion of GNPs in this study. The concentration of the GNP solution used was 1 g/L.

Mechanical methods (shear blending and ultrasonic vibration) are frequently used to break the van der Waals bonds of graphene flakes in solutions [37]. Because of the ease of operation, a bath-type ultrasonic vibrator (Model WC-650 from Conjutek) was used for graphene dispersion in this study. The degree of graphene dispersion depends on the power, frequency, and duration of ultrasonic vibration [35]. In this study, the frequency and power of ultrasonic vibration were 40 kHz and 650 W, respectively.

The prepared graphene solutions were subjected to ultrasonic vibration for specific sonication times. The sonication times were 15, 30, 45, and 60 min for the GO solution and 5, 10, 15, 20, 25, 30, 35, 40, 45, 50, 55, and 60 min for the GNP solution. The appearance of the graphene solutions after ultrasonic vibration is shown in Fig. 2(a). The solutions containing dispersed graphene were black and turbid, and graphene was uniformly dispersed in these solutions to a certain extent. After the solutions were left standing for a certain time, graphene agglomerated and began to settle at the bottom of the test tubes containing the solutions. To determine the degree of graphene dispersion, a hydrometer was placed in the dispersed suspension solutions to measure their specific gravity values, as displayed in Fig. 2(b). The specific gravity ranges measured by using the hydrometer for the GO and GNP solutions were 0.995–1.050 and 0.760–0.820, respectively. Fig. 2(b)–2(e) depict the specific gravity values of the solutions measured at different precipitation times (t), beginning from t = 0 until the graphene completely settled at the bottom of a graduated cylinder. When all graphene flakes settled at the bottom of the solution, the specific gravity of the solution became constant. The settling time refers to the earliest time at which the specific gravity of the solution no longer changes. The longer the settling time of the solution, the longer graphene takes to

(a) Graphene oxide (GO) (b) Multilayer graphene platelets (GNPs)

Fig. 1. The SEM images of GO and GNPs. (Courtesy of Conjutek Corporation).

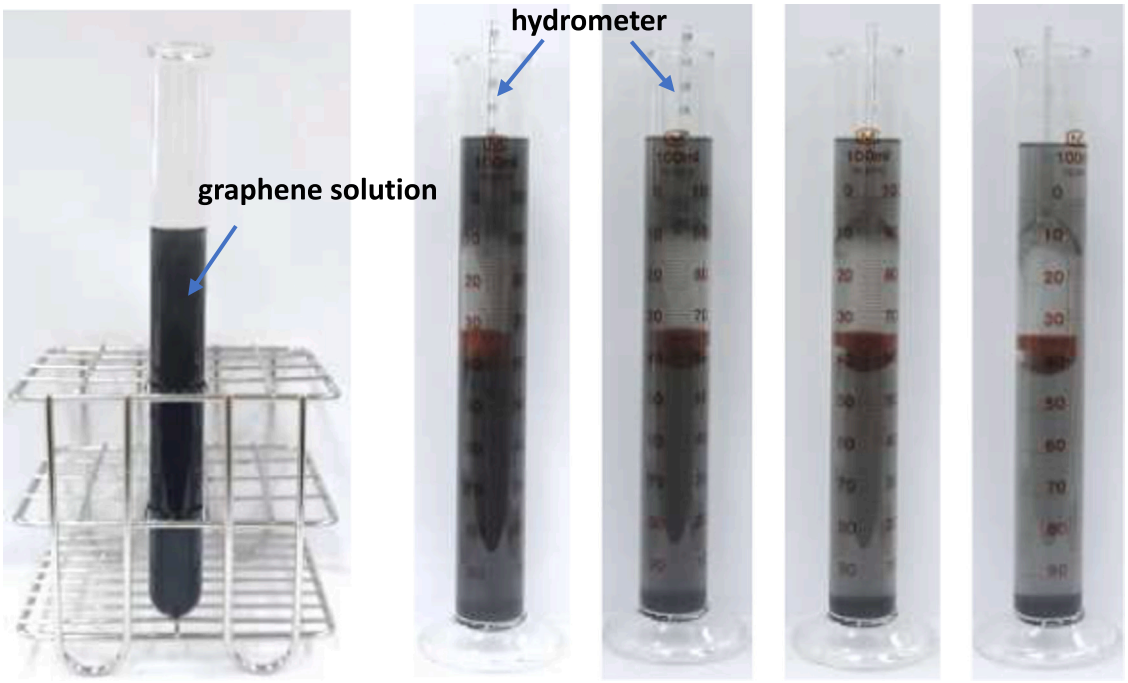

Fig. 2. Changes in the specific gravity of a solution of GNPs measured using a hydrometer: (a) GNP solution obtained after ultrasonic vibration and specific gravity measurements at precipitation times (t) of (b) 0, (c) 6, (d) 12, and (e) 48 h.

complete reagglomeration, and thus, the higher the dispersibility of graphene. Fig. 3 shows the relationship between the settling time and the sonication time. The optimal sonication times for the dispersion of GO in water and that of GNPs in ethanol were 30 and 15 min, respectively.

2.3. Specimen preparation

Graphene solutions sonicated for the optimal time were mixed with the PZT/cement composite. To find the optimal graphene content for enhancing the piezoelectric properties of the composites, specimens containing GO were prepared by employing a dry-mixing method. The GO content of these samples was 0.1–0.5% by the volume of cement. The dry-mixing method was used to dry the dispersed graphene solutions in an oven, and then, the dispersed graphene was added to the cement and PZT powders. The graphene mixtures containing GO were initially stirred manually and then rotated clockwise and counterclockwise in a planetary ball mill at 100 rpm for 5 min. Wet-mixing was performed for the specimens containing GNPs, wherein the GNP content was 0.1–0.9%. The wet-mixing method involved pipetting out a specific content of dispersed graphene solution and adding it to a mixture of cement and PZT, as shown in Fig. 4. The graphene mixtures containing GNPs were manually mixed, and ethanol was added to them. The resultant mixture was then placed in a porcelain bowl (mill cup), as displayed in Fig. 5, and spun in a planetary ball mill at 100 rpm for 5 min. The effects of dry- and wet-mixing on the piezoelectric properties of the adopted composite with the optimum graphene content were investigated. A flow chart of manufacturing process is shown in Fig. 6.

The optimal GNP content was determined by comparing the maximum values of d_{33} and ε_r for the different graphene composites.

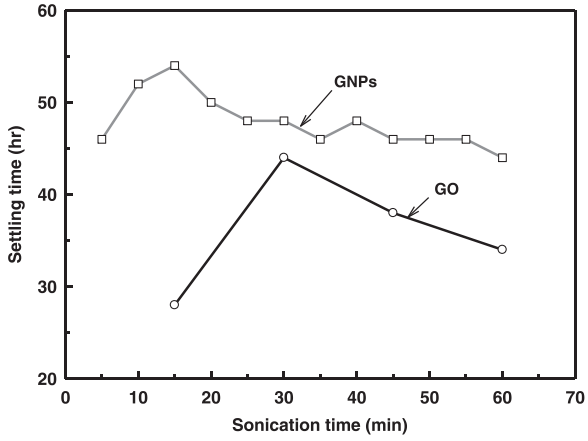

Fig. 3. Settling time versus sonication time for the solutions of GO in water and GNPs in ethanol.

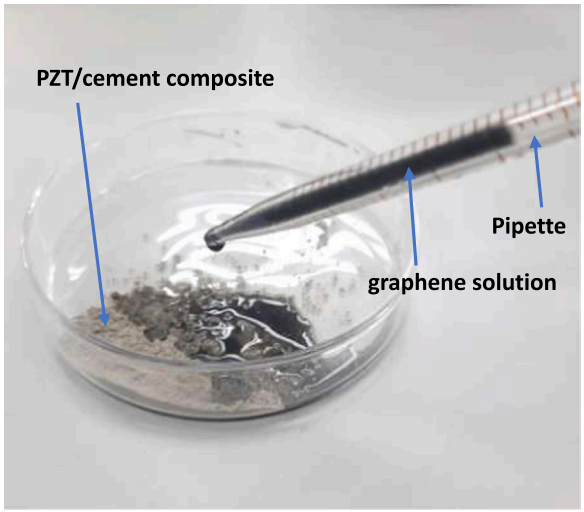

Fig. 4. Graphene solution added to the PZT/cement composites (wet mixing).

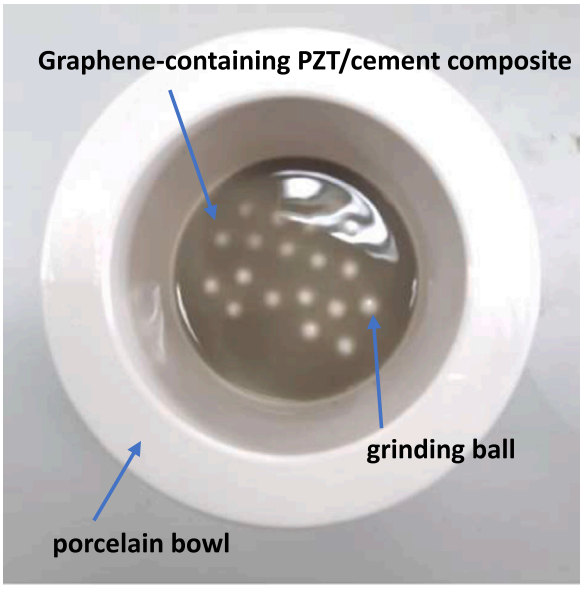

Fig. 5. Dispersal of the GNP-containing PZT/cement composite in a porcelain bowl by using a planetary ball mill.

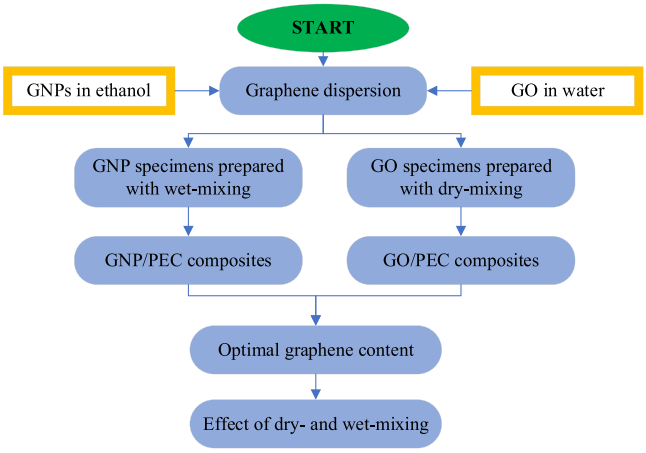

Fig. 6. Flow chart of manufacturing process.

First, solutions of GNPs and ethanol (symbol GN) and GNPs and ethanol containing a superplasticizer (symbol GS) were prepared and subjected to ultrasonic vibration, shown in Table 3. The adopted superplasticizer met the ASTM C494 type F specifications and had a specific gravity of 1.03–1.09 g/mL. The dispersed solutions of GN and GS were dry-mixed and wet-mixed with the PZT/cement composite to fabricate GNP/PEC composite specimens. GND and GNW represent the dry- and wet-mixed specimens of the composite by using the GN solution, respectively. GSW denotes the composite created via wet-mixing by using the GS solution. The control samples are PEC samples (without graphene addition), and PEC-D and PEC-W represent the PEC composites produced through dry- and wet-mixing (in ethanol), respectively.

After the raw materials were mixed, the mixtures were placed in a steel mold having a diameter of 15 mm to form disks. The specimens were then fabricated by applying a pressure of 80 MPa to the mixture and maintaining the pressure for 5 min. The pressed specimens were cured at a temperature of 90 °C and a relative humidity of 100% for 24 h to ensure that they developed high forming strength. After curing, the specimens were polished to a thickness of 2 mm and air-dried at 25 °C for 1 h. Electrodes were created on the specimens by coating the two sides with conductive silver paste (SYP-4570).

Table 3
Symbol for the GNP solutions.

Solution	Solvent	Superplasticizer	GNP concentration	Vibration time
GN	Ethanol	None	1 g/L	15 min
GS	Ethanol	1% solvent (by volume)	1 g/L	15 min

For PEC composites, the double heat treatment method effectively increases d_{33} and ε_r [56]. In this method, the specimen was heated at 140 °C for 40 min before and after electrode fabrication. In this manner, the dielectric loss, *D,* of the specimen can be considerably reduced and the polarization efficiency during polarization can be improved, thus enhancing the piezoelectric properties of the specimen. Therefore, the specimens were subjected to double heat treatment prior to polarization. The electric properties of the specimens were determined prior to polarization.

2.4. Specimen polarization and measurement

After the double heat treatment was employed, the specimens were subjected to an electric field of 1.5 kV/mm at 150 °C (poling temperature) for 40 min (poling time). Most of the piezoelectric and electrical properties of the specimens were measured directly by using a d_{33} piezometer (Model P/N 90–2030) and an impedance phase analyzer (Model 6520); then, ε_r, electromechanical coupling coefficient k_t, and resistivity ρ were calculated. The dielectric loss, *D,* and resistance, *R,* of the specimen were measured at 1 kHz and 1 V, and d_{33} was measured at 110 Hz.

The relative permittivity (relative dielectric constant), ε_r, was discussed [73] and calculated using the following equation [52]:

$$\varepsilon_r = \frac{Ct}{A\varepsilon_0}, \tag{1}$$

where t represents the specimen thickness, A represents the electrode area (ϕ15 mm × 2 mm in this study), C is the capacitance measured at 1 kHz, and $\varepsilon_0 = 8.854 \times 10^{-12}$ F/m is the vacuum permittivity. The k_t value was determined using the following formula [74]:

$$k_t^2 = \frac{\pi}{2}\frac{f_m}{f_n}\tan\left(\frac{\pi}{2}\frac{f_n - f_m}{f_n}\right), \tag{2}$$

where f_m and f_n are the resonance frequencies at the minimum and maximum impedances, respectively, in the impedance–frequency spectrum of the specimens. Resistivity ρ was calculated using the following equation:

$$\rho = \frac{RA}{L}, \tag{3}$$

where R is the resistance, and L is the length (t in this study) of the specimen. The piezoelectric voltage coefficient, g_{33}, was calculated using the following equation [75]:

$$g_{33} = \frac{d_{33}}{\varepsilon_r\varepsilon_0}, \tag{4}$$

where d_{33} is piezoelectric charge coefficient (pC/N), ε_r is relative permittivity, and ε_0 is vacuum permittivity (8.854 pF/m).

All data were measured from 24 h (day 1) to 100 d after polarization. The temperature and humidity levels in the measurements were maintained at 24 ± 1 °C and 50%, respectively. The values presented for each parameter in this study represent the average of the values obtained for the three specimens. Additionally, the d_{33} value of the specimen was determined as the average of the d_{33} values at nine points on the specimen.

3. Results and discussion

3.1. Effects of GO on the piezoelectric properties

The specimens prepared through dry-mixing were subjected to a double heat treatment. The resistivity (ρ) values of the PEC containing 0–0.5% GO before and after polarization were calculated using Eq. 3, and the results are shown in Fig. 7. Before polarization, the resistivity of the GO-containing PEC composites increased considerably from 60.1 kΩ·m at a GO content of 0% to 89.4 kΩ·m at a GO content of 0.1%. This result was obtained because the oxygen functional groups in GO enhanced the insulating properties of PEC. When the GO content increased to 0.5%, the ρ value increased to 93.1 kΩ·m. Although the ρ value could be increased by increasing the GO content, the most efficient ρ increase was achieved when the GO content increased from 0% to 0.1%. The alignment of electrons is not easily accomplished in high-resistance materials during polarization, resulting in an inefficient polarization. Therefore, a greater difficulty might be faced when polarizing a cementitious material with a higher GO content. Consequently, the material with a higher GO content exhibits lower piezoelectric properties. In this study, the ρ values after polarization were lower than those before polarization. After polarization, the electrons of the PEC were aligned along the poling direction, which increased its conductivity (and decreased its resistivity).

The dielectric loss can be used as an index to evaluate the difficulty of material polarization. The D value of PZT/cement composites should preferably be less than 0.75 before polarization to ensure the feasibility of polarization [57,76]. Fig. 8 displays the D values of the specimens before and after polarization. Before polarization, the D value increased from 0.14 at a GO content of 0% to approximately 0.24 at a GO content of 0.5%. Thus, the addition of GO increased the difficulty of material polarization and easily caused specimen breakdown. During polarization, the time to reach the poling voltage (trigger time) was longer for specimens containing GO than for that without GO. Nevertheless, the GO-containing specimens could be polarized to enable them to acquire piezoelectric properties. In addition, after polarization, the dielectric loss D increased with time and plateaued at approximately 50–60 d. The D values of the specimens 100 d after polarization are presented in Fig. 8, which indicates that the dielectric loss of the specimens containing GO was smaller than that of the specimen without GO. Thus, the filling effect of GO in cement reduces the leakage currents of polarized PZT/cement composites.

The relative permittivity ε_r was calculated from the capacitance (C) values measured before and after polarization by using Eq. 1 (Fig. 9). Before polarization, the ε_r value of the specimens containing GO was marginally lower than that of the specimen without GO. The ε_r values of the composites containing 0% and 0.3% GO were 49 and 40, respectively. Thus, the addition of GO to PZT/cement composites marginally reduced their ability to store electrical energy (i.e., power storage capacity). After polarization, the ε_r value increased with time and plateaued at approximately 30–40 d. For the composite containing 0% GO, the ε_r values before polarization and 100 d after polarization were 49 and 444, respectively (Fig. 9). For the aforementioned composite, the ε_r value increased considerably after polarization owing to the effect of the functional PZT particles. However, 100 d after polarization, the ε_r value decreased considerably with an increase in the GO content. For instance, the ε_r value decreased to 270 for the GO content of 0.1%. This result was possibly because the D value before polarization increased with increasing GO content (Fig. 8), which resulted in decreasing polarization efficiency and, thus, the ε_r value. Therefore, a high GO content is not conducive to increasing the relative permittivity of cementitious materials after polarization.

PZT/cement composites do not exhibit piezoelectric properties until they are polarized. The piezoelectric charge coefficient d_{33} and electromechanical coupling coefficient k_t of the GO/PEC composites 100 d after polarization are shown in Fig. 10. The d_{33} value of the composite without GO was 98 pC/N, and the d_{33} value decreased with an increasing GO content. For example, the d_{33} value was 49 pC/N when the GO content was 0.1%. Thus, the d_{33} value decreased by 50% as the GO content increased from 0% to 0.1%. When the GO content increased to 0.5%, the d_{33} value decreased to 24 pC/N. The variations in d_{33} with the GO content were similar to those in ε_r after polarization with the GO content (Fig. 9). This result was possibly because the oxygen functional groups of GO increased the electrical resistance (Fig. 7) and dielectric

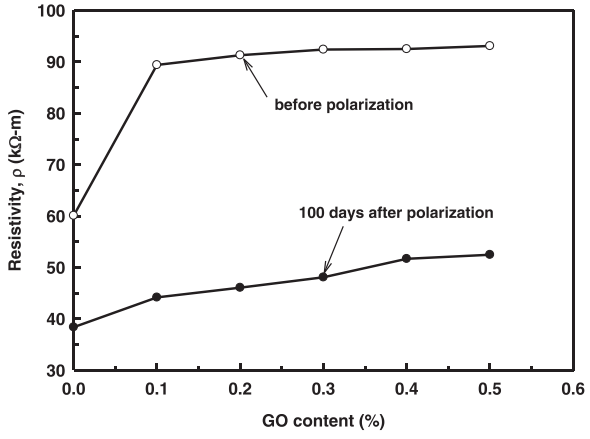

Fig. 7. The resistivity versus the GO content before and after polarization.

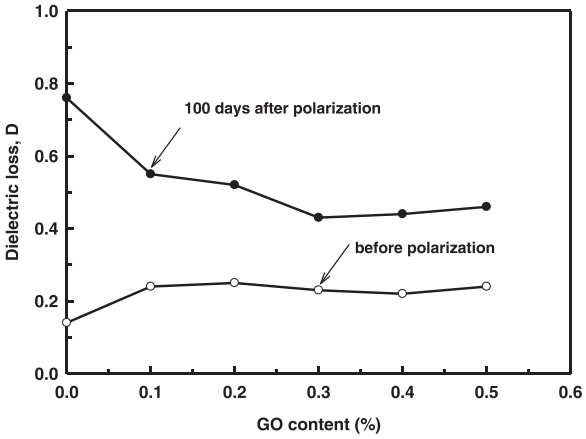

Fig. 8. The dielectric loss versus the GO content before and after polarization.

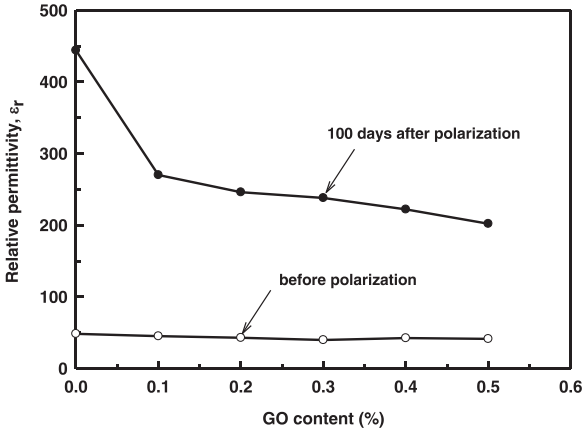

Fig. 9. The relative permittivity versus the GO content before and after polarization.

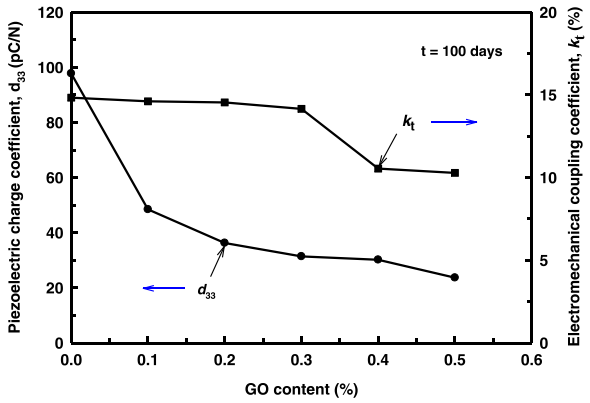

Fig. 10. Effects of the GO content on the piezoelectric charge coefficient d_{33} and electromechanical coupling coefficient k_t.

loss (Fig. 8) of the material before polarization, thereby reducing the polarization efficiency. Thus, compared with the specimen without GO, the specimens containing GO had longer trigger times (excitation times) and worse electron alignment in the poling direction, and thus, lower d_{33} values. For use as piezoelectric sensors and actuators, cementitious composites must have suitable piezoelectric properties, particularly high d_{33} values. The addition of GO reduces the d_{33} value of PEC materials, which results in a decrease in the piezoelectric sensitivity of the sensors developed using these materials.

Fig. 10 also presents the k_t values calculated using the impedance–frequency spectrum and Eq. 2. Between the GO contents of 0% and 0.3%, k_t decreased marginally from 0.148 to 0.142. However, when the GO content was 0.4%, the k_t value decreased considerably to 0.106. The k_t value at a GO content of 0.5% was 31% lower than that at a GO content of 0%, which indicated that the addition of GO resulted in a decrease in the electromechanical coupling coefficient of the PEC. The GO-containing PEC composites were observed 90 d after polarization using a scanning electron microscope at 5000 × magnification (Fig. 11). A scanning electron microscopy image of the specimen without GO is shown in Fig. 11(a). This image indicates that the specimen contained hydration products (such as CH and C–S–H), PZT, and pores. Some pores existed in the interfacial transition zone between the cement and PZT, and in the hydration product zone. An SEM image of the specimen containing 0.1% GO is shown in Fig. 11(b). This image is similar to that shown in Fig. 11(a) (i.e., some pores can be clearly observed). For the specimens with 0.2% and 0.3% GO, a few pores were present in the overall structure. The pore size and number of pores were considerably smaller for the specimen containing 0.2% GO [Fig. 11(c)] than for the specimens containing 0% and 0.1% GO [Fig. 11(a) and 11(b), respectively]. The specimen with a GO content of 0.4% [Fig. 11(d)] exhibited a compact structure (i.e., compacted growth of hydration products was observed), and only a few small pores were observed in the interfacial transition zone. This observation is similar to the results of Chintalapudi et al. [28] and Li et al. [33], who found that the addition of GO could

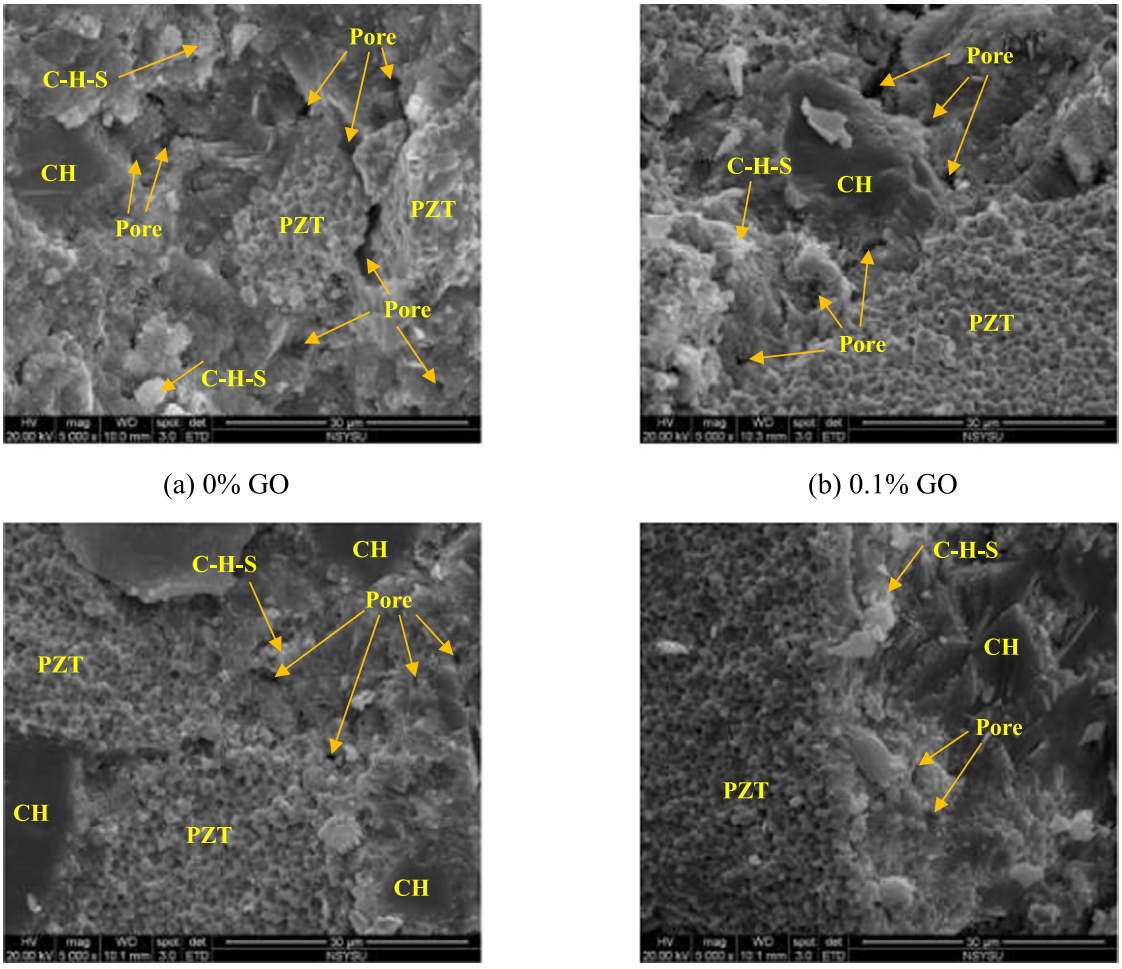

Fig. 11. SEM images for the GO/PEC composites containing (a) 0%, (b) 0.1%, (c) 0.2%, and (d) 0.4% GO.

reduce cement porosity and prevent crack propagation, thereby improving the mechanical properties of cementitious composites. In addition, according to experimental observations [57], an appropriate porosity in cement can improve the electromechanical coupling coefficient of the PEC. Therefore, the decrease in the k_t value with increasing GO content can be attributed to the decrease in the porosity of cementitious materials with increasing GO content.

3.2. Optimal GNP content

The GNP and PZT/cement composites were wet-mixed in ethanol to prepare the specimens (GNP/PEC composites) and subjected to double heat treatment. The GNP content of the GNW specimens was 0.1–0.9%, and the specimen without GNPs was denoted as PEC-W. After the specimens were polarized, their d_{33} and ε_r values were measured to determine the optimum GNP content for the GNP/PEC composites.

Fig. 12 shows the d_{33} value of the GNP-containing PEC composites 90 days after polarization. The d_{33} value initially increased with the GNP content and then decreased when the GNP content exceeded 0.3%. The highest value of d_{33} was 117 pC/N at a GNP content of 0.3%. The d_{33} value was 18% higher than that of the PEC-W (d_{33} = 99 pC/N). The aforementioned trend of d_{33} is similar to that obtained by Gong et al. [65] when CNTs were added to a 0–3-type cement composite. Gong et al. [65] reported that when the CNT content was between 0% and 0.3%, the d_{33} value increased with an increasing CNT content. However, when the CNT content exceeded 0.3%, the d_{33} value decreased with increasing CNT content. Gong et al. [65] concluded that an appropriate amount of CNTs can improve the piezoelectric and electrical properties of cement-based composites. However, using an excessive amount of carbon nanomaterials increases the dielectric loss of these composites and causes leakage currents. The generated leakage current dissipates some electrical energy during polarization; thus, the polarization cannot be effectively completed. Therefore, the D value of the GNP/PEC composites increases under excessive GNP addition, which reduces the polarization efficiency and, thus, the d_{33} value. In this study, the optimum GNP content was 0.3%, which was similar to the optimal CNT content for the 0–3-type cement composite. The relative permittivity ε_r of the GNP-containing PEC composites 90 d after polarization is displayed in Fig. 13. Similar to the trend observed for d_{33}, the ε_r value first increased and then decreased with increasing GNP content. A maximum ε_r value of 588 occurred when the GNP content was 0.3%. This ε_r value is 17% higher than that of the PEC-W specimen (ε_r = 502). Thus, in response to Jaitanong et al. [70], the optimal GNP content for enhancing the dielectric constant was determined. Materials with high ε_r values have high charge storage capacities. The addition of appropriate amounts of GNPs can increase the electricity storage capacity of cementitious materials with an optimal GNP content of 0.3%. As displayed in Figs. 12 and 13, the PEC composites with 0.3% GNPs exhibit the highest

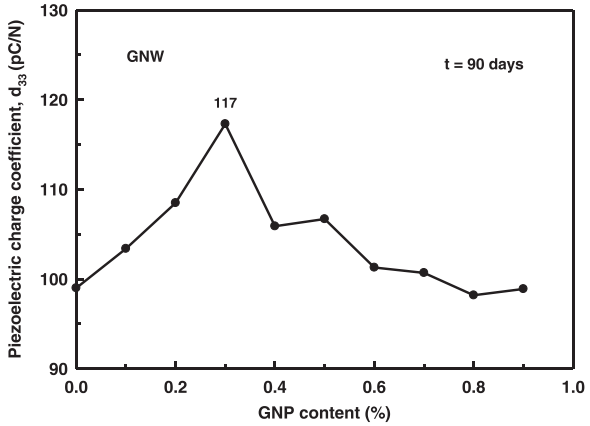

Fig. 12. The piezoelectric charge coefficient versus the GNP content.

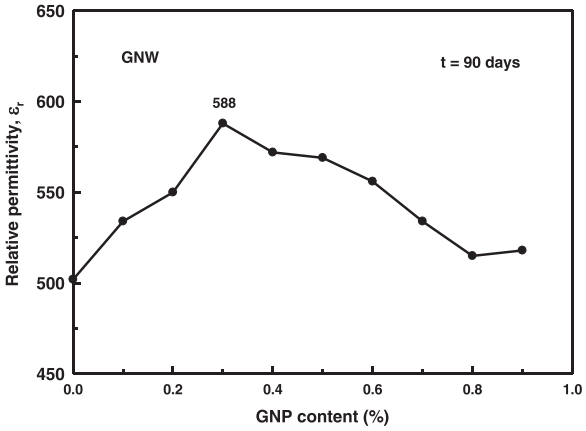

Fig. 13. The relative permittivity versus the GNP content.

piezoelectricity. Thus, the addition of appropriate amounts of GNPs can improve the piezoelectric properties of cementitious materials.

As the structural health monitoring sensor, the piezoelectric voltage coefficient g_{33} is an important property. The g_{33} value of the PEC composites containing GO and GNPs at 90 days is listed in Table 4. The g_{33} values of GO/PEC composites decreased with increasing GO content, indicating that adding GO to the composites adversely affects the application in structural health monitoring. However, the g_{33} values of the composites containing GNPs in the range of $20.6 - 22.5 \times 10^{-3}$ V·m/N are favorable for use in SHM. When the GNPs content is 0.3%, the maximum value of g_{33} reaches 22.5×10^{-3} V·m/N.

3.3. Effects of GNP mixing

To study the effects of GNP mixing, the optimal GNP content (0.3%) was dry-mixed and wet-mixed with the PEC composite to prepare GND, GNW, and GSW specimens. PEC-D and PEC-W specimens, which did not contain GNPs, served as controls for comparison.

The pore distributions of the GNP-containing PEC composites were examined using an optical microscope at 350× after curing the composites for 24 h. Optical microscopy (OM) images of the composites were input into PIA image analysis software to locate the composite pores. This software highlights pores in red in the OM images by selecting a pixel threshold criterion of 100 (Fig. 14). The aforementioned software uses a grayscale value to estimate the porosity of a specimen surface. Fig. 15 presents the porosity values of the GNP/PEC composites. The addition of GNPs to the PEC specimens reduced their porosities. The wet-mixed specimens (PEC-W, GNW, and GSW) in ethanol had lower porosities than the dry-mixed specimens (PEC-D and GND).

The GNP-containing PEC composites were also analyzed by SEM, as shown in Fig. 16. Most of the pores of the PEC-D and PEC-W specimens [Fig. 16(a) and 16(b), respectively] existed near the interface between the PZT and cement. Fig. 16(c)–16(e) depict the SEM images of the specimens containing GNPs, which are irregular flakes that are stacked together and fill the voids in the interfacial transition zone. The SEM images indicated that the pore sizes of the dry-mixed specimens (PEC-D and GND) were larger than those of the wet-mixed specimens (PEC-W, GNW, and GSW). In particular, the GSW specimen exhibited the smallest pore size [Fig. 16(e)] and lowest porosity (Fig. 15). Moreover, the carbon content at locations denoted by red squares in Fig. 16(c)–16(e) was measured using energy-dispersive X-ray (EDX) spectroscopy, and the results are listed in Table 5. The carbon content of the GNPs (multilayer graphene) varied in different specimens, which might be attributed to GNP agglomeration. The higher the number of layers in a multilayer graphene stack (agglomeration), the higher is the carbon content. This result might be related to the dispersion of GNPs and their mixing with

Table 4
The g_{33} value of PEC composites containing GO and GNPs at 90 days. ($\times 10^{-3}$ V·m/N).

Content	0%	0.1%	0.2%	0.3%	0.4%	0.5%	0.6%	0.7%	0.8%	0.9%
GO[a]	24.9	20.3	16.7	14.9	15.4	13.3	–	–	–	–
GNPs[b]	22.3	21.9	22.3	22.5	20.9	21.2	20.6	21.3	21.5	21.6

[a] Note: The GO/PEC composites were dry-mixing.
[b] Note: The GNP/PEC composites were wet-mixing.

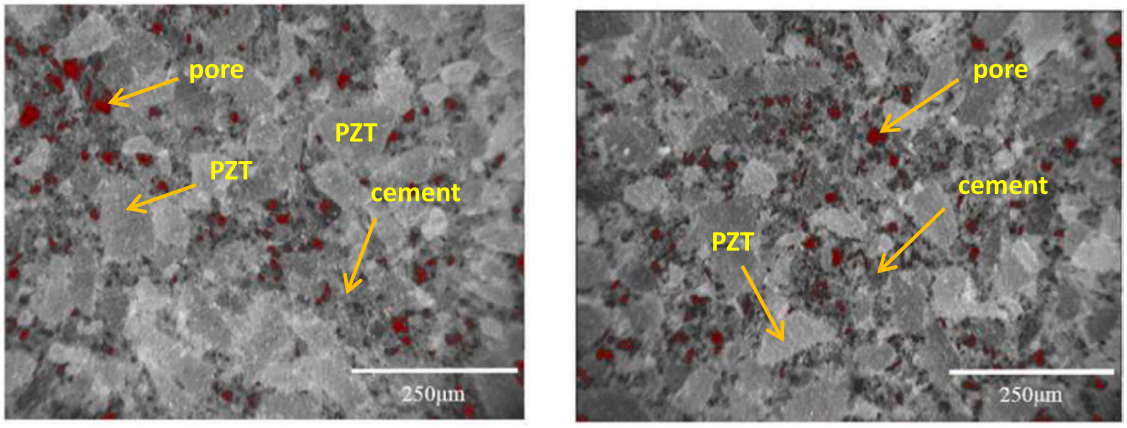

(a) PEC-D specimen (b) GSW specimen

Fig. 14. OM images of the PEC-D and GSW specimens (these images display the distributions of pores, cement and PZT particles in the specimens).

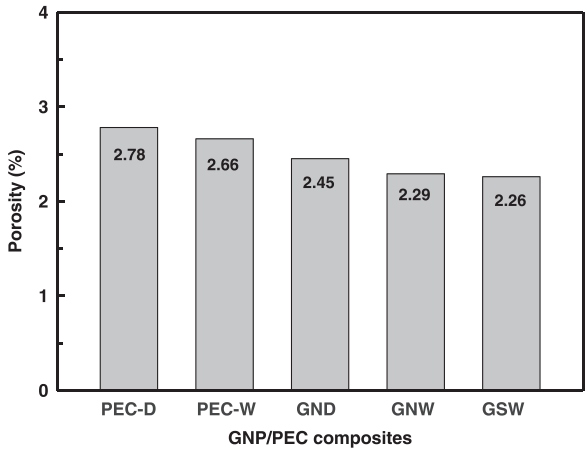

Fig. 15. Effect of the mixing method on the porosity of the GNP/PEC composites containing 0.3% GNPs.

the cementitious materials. The carbon content in Zone 1 of the GND specimen [Fig. 16(c)] was low (2.15% C), and the material in this zone did not appear to be graphene. However, the carbon content in Zones 2, 3, and 4 (Table 5) was relatively high; therefore, the specimen was composed of graphene. The carbon content of the GND and GNW specimens was 85.79% (Zone 2) and 50.21% (Zone 3), respectively. These results indicate that agglomeration (stacked flakes) of GNPs in the PEC specimens can be reduced by applying wet-mixing. When a superplasticizer was added to the GNP solution, the carbon content of the GSW specimen was 35% (Zone 4), which was 15.21% lower than that of the GNW specimen (Zone 3). Therefore, GNPs were dispersed in ethanol and a superplasticizer (1%) and mixed with a cementitious material (PEC) through wet-mixing, which could reduce the agglomeration of GNPs in PEC.

The ρ values of the GNP/PEC composites containing 0.3% GNPs before and after polarization are shown in Fig. 17. The specimens containing GNPs (GND, GNW, and GSW) had lower ρ values than those without GNPs (PEC-D and PEC-W) before and after polarization. For instance, before polarization, the resistivity of the GNW specimen ($\rho = 53.8$ kΩ·m) was the lowest among all the specimens. The ρ value of the GNW specimen was 10.9% lower than that of the PEC-D specimen ($\rho = 60.4$ kΩ·m), which did not contain GNPs. This result is consistent with that of Bai et al. [21], who reported that graphene addition to cement can reduce the resistivity of cement composites. The PEC-D and PEC-W specimens exhibited resistivity values of 60.4 and 58.1 kΩ·m, respectively (a difference of 3.81%). This result indicates that the addition of GNPs and the wet-mixing method can reduce the ρ value (increase the conductivity) of the PZT/cement composites. Cementitious materials with a lower resistance can be polarized more easily. Therefore, the addition of GNPs is helpful for polarizing the PZT/cement composites. In this study, the GNP/PEC composites exhibited similar decreasing trends in resistance before and after polarization. In contrast to the addition of GO (Fig. 7), the addition of GNPs reduced the electrical resistance of the cementitious materials because GNPs are conductive materials (Table 2), whereas GO is not. The resistance of the wet-mixed specimens, especially GSW after polarization (Fig. 17), was lower than that of the dry-mixed specimens.

The D values of the GNP/PEC composites are shown in Fig. 18. Before polarization, the D values of the specimens containing GNPs were higher than those of the specimens without GNPs. For example, the dielectric loss of the GND specimen was 0.17, which is 21.4% higher than that of the PEC-D specimen ($D = 0.14$). The D value of the GSW specimen ($D = 0.21$) was 31.3% higher than that of the PEC-W specimen ($D = 0.16$). Jaitanong et al. [70] obtained similar results as the aforementioned ones and found that the dielectric loss of the silica/cement binder increased with the addition of GNPs. The addition of GNPs increased the D value (resulting in a higher leakage current) and thus, the difficulty of material polarization. This result was similar to that obtained for GO (Fig. 8). The maximum D value was 0.21 before polarization (Fig. 18), which is smaller than 0.75 [57,76] and within the polarizable range for obtaining suitable piezoelectric properties. In addition, after polarization, the D values of the GNP-containing composites were higher than those of the

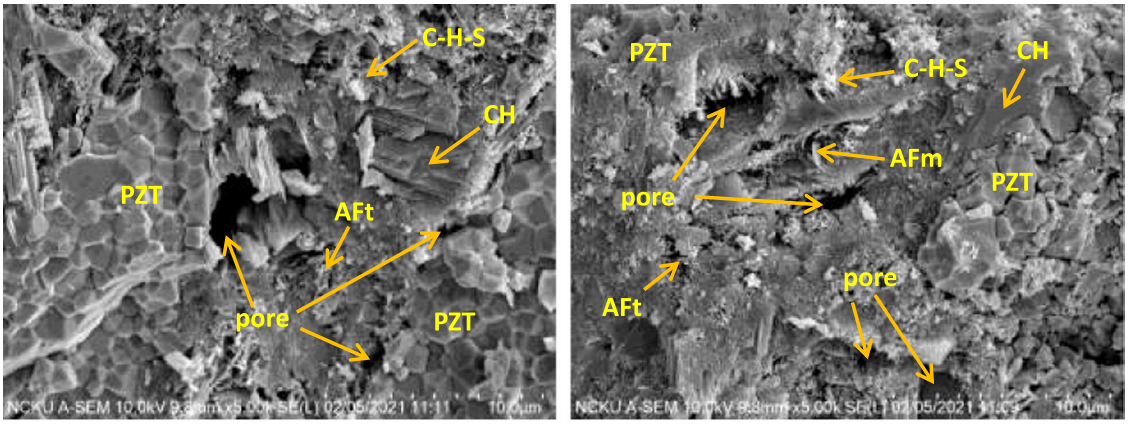

(a) PEC-D specimen (b) PEC-W specimen

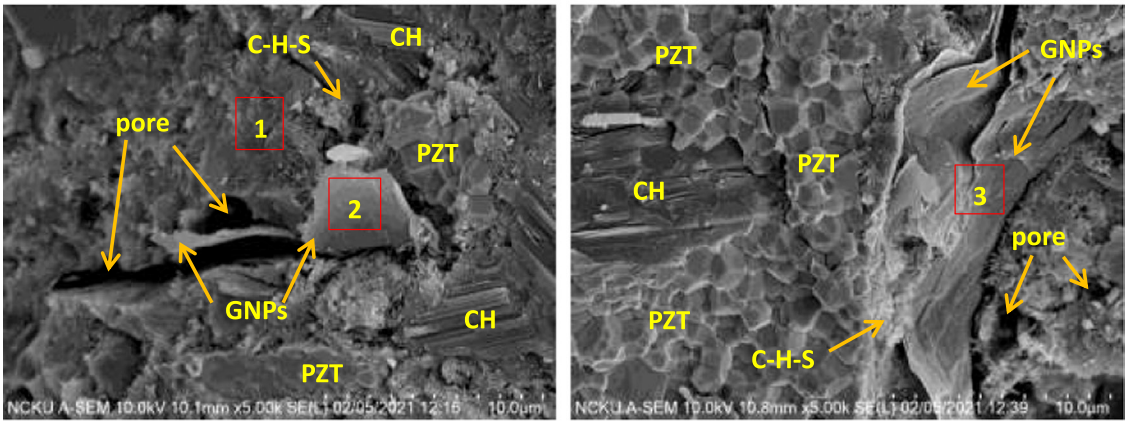

(c) GND specimen (d) GNW specimen

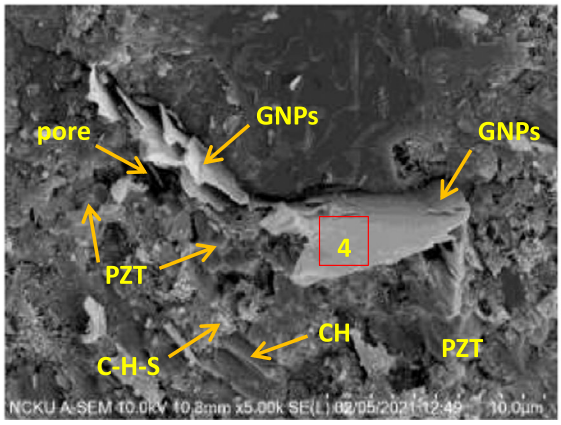

(e) GSW specimen

Fig. 16. SEM images of the GNP/PEC specimens after curing at 90 ℃ for 24 h.

Table 5
Carbon content measured through EDX.

	GND		GNW	GSW
Position	Zone 1	Zone 2	Zone 3	Zone 4
C (%)	2.15	85.79	50.21	35.00

PEC composites. This result can be attributed to the absorbed moisture, PZT particles and the conductivity of GNPs.

Fig. 19 illustrates the relative permittivity of the examined specimens. The addition of appropriate amounts of GNPs and the use of wet-mixing increased the ε_r values before and after polarization. Before polarization, the ε_r value (= 60) of the GSW specimen was 22.4% higher than that of the PEC-D specimen ($\varepsilon_r = 49$). The ε_r values of the dry-mixed specimens with 0.3% GNPs (GND in Fig. 19) and 0.3% GO (Fig. 9) were 53 and 40, respectively. These results indicate that GNP addition is

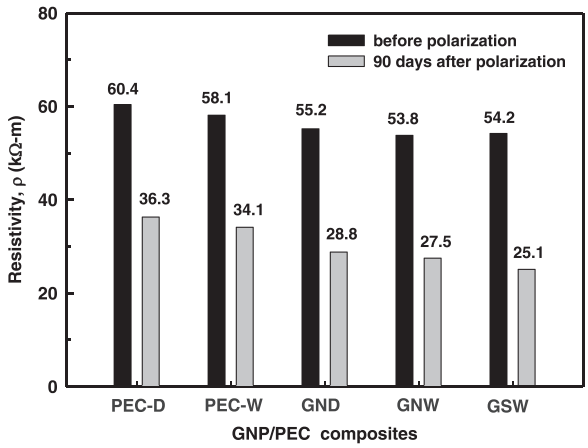

Fig. 17. Effect of the mixing method on the resistivity of the GNP/PEC composites containing 0.3% GNPs.

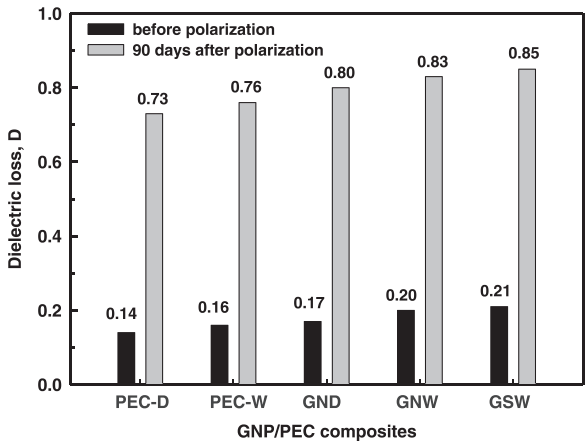

Fig. 18. Effect of the mixing method on the dielectric loss of the GNP/PEC composites containing 0.3% GNPs.

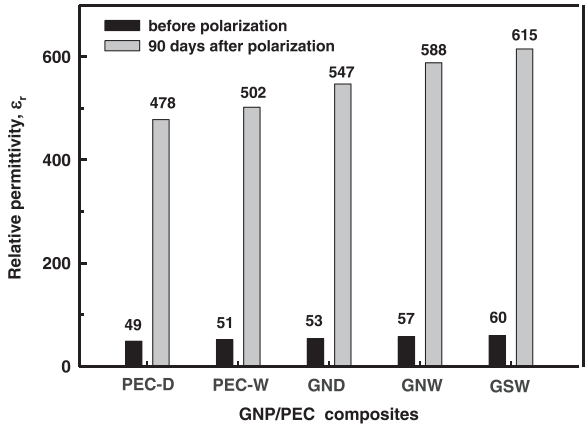

Fig. 19. Effect of the mixing method on the relative permittivity of the GNP/PEC composites containing 0.3% GNPs.

superior to GO addition in terms of increasing the ε_r value. Similarly, the relative permittivity of the PEC composites after polarization was higher when GNPs were used than when GO was used. Thus, the addition of GNPs can considerably enhance the relative permittivity after polarization. Wet-mixing can increase ε_r to a greater extent than dry-mixing can. In this study, the GNP/PEC piezoelectric composite with a superplasticizer (GSW specimen) exhibited the highest ε_r value of 615.

The piezoelectric charge coefficient of cementitious materials increased with time after polarization [14,76]. The d_{33} values of the composites without GNPs were nearly constant approximately 30–40 d after polarization, whereas those of the composites with GNPs were nearly constant approximately 50–60 d after polarization. Fig. 20 depicts the d_{33} values of the GNP/PEC composites 90 d after polarization. The addition of GNPs increased the d_{33} and, thus, the sensitivity of the PZT/cement composite as a piezoelectric sensor. The GSW specimen exhibited the highest sensitivity as a sensing element, possibly because the use of a superplasticizer resulted in multilayer graphene with high dispersibility. The d_{33} values of the GNW and GSW specimens were 19.4% (d_{33} = 117 pC/N) and 25.5% (d_{33} = 123 pC/N) higher, respectively, than that of the PEC-D composite (d_{33} = 98 pC/N). The optimal piezoelectric constant d_{33} of 123 pC/N can be obtained at 90 days for GSW in GNP/PEC composite. This d_{33} value is higher than the d_{33} values reported in the literature for piezoelectric PZT/cement composites containing 50% PZT [66]. The effect of the mixing method on g_{33} is shown in Table 6. The GNP mixing method has a slight effect on g_{33}. The g_{33} values of the GNP/PEC composites containing 0.3% GNPs are in the range of 22.5–22.9 $\times$ 10^{-3} V·m/N close to that of PZT ceramic material (g_{33} =24 $\times 10^{-3}$ V·m/N).

As shown in Fig. 10, the electromechanical coupling coefficient marginally decreases with the addition of 0.3% GO. The k_t values of the GNP/PEC composites are presented in Fig. 21. The k_t values of the PEC specimens containing GNPs are higher than those of the PEC specimens without GNPs. When 0.3% GNPs and a superplasticizer are wet-mixed with PEC, the k_t value increases from 0.147 (for the specimen without GNPs) to 0.202, representing an increase of approximately 37.4%. Therefore, the appropriate amounts of GNPs can effectively increase k_t and, thus, increase the energy conversion efficiency. Thus, GNP-containing piezoelectric cementitious materials have the potential to be utilized as energy-harvesting materials.

4. Conclusions

In this study, the effects of the addition of GO and GNPs through dry- and wet-mixing on the piezoelectric properties of PZT/cement composites containing 50% PZT and 50% cement were examined. These composites can be used to fabricate sensing elements for piezoelectric sensors. GO and GNPs were dispersed in pure water and ethanol, respectively. The settling times of the graphene solutions were determined using a hydrometer. Experiments indicated that sonication times of 30 and 15 min resulted in the optimal dispersion of GO and GNPs, respectively. The addition of GO and GNPs increased the dielectric loss of the examined composites, thereby increasing the difficulty in

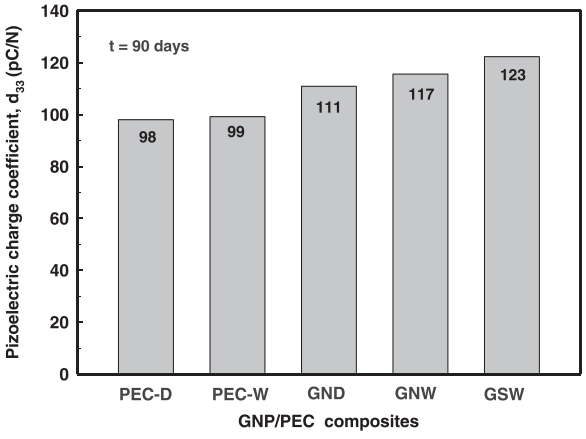

Fig. 20. Effect of the mixing method on the piezoelectric charge coefficient of the GNP/PEC composites containing 0.3% GNPs.

Table 6
Effect of the mixing method on the g_{33} of PEC composites containing 0.3% GNPs. ($\times 10^{-3}$ V·m/N).

PEC composite		GNP/PEC composite		
PEC-D	PEC-W	GND	GNW	GSW
23.2	22.3	22.9	22.5	22.6

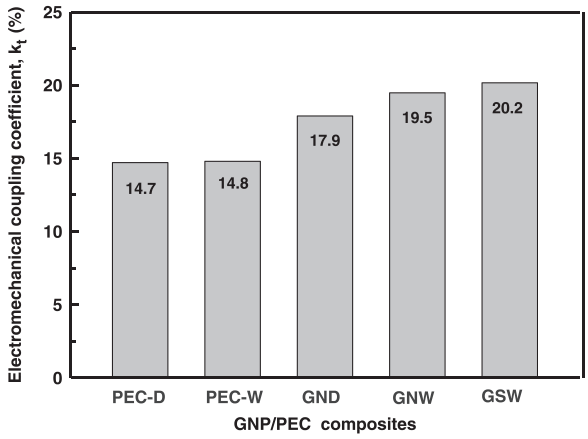

Fig. 21. Effect of the mixing method on the electromechanical coupling coefficient of the GNP/PEC composites containing 0.3% GNPs.

polarizing the composites. Nevertheless, the composites could be polarized, which allowed them to exhibit piezoelectric properties. The addition of GO negatively affected the piezoelectric properties by resulting in a decrease in piezoelectric charge coefficient d_{33}, piezoelectric voltage coefficient g_{33}, relative permittivity ε_r, and electromechanical coupling coefficient k_t. These results may be attributed to the insulating properties of GO. The addition of GO increased the dielectric loss and resistivity of the composites before polarization, which increased the leakage current and dissipation of the stored energy in the composites during polarization. A low polarization efficiency leads to poor piezoelectric properties. The addition of GNPs reduced the resistance of the composites because of the high electrical conductivity of GNPs. The piezoelectric properties of the composites, including their ε_r and d_{33} values, were satisfactory when the GNP content was 0.1–0.5%. The maximum ε_r and d_{33} values were obtained when the GNP content was 0.3%. The wet-mixing of GNPs and PZT/cement composites with ethanol yielded superior piezoelectric properties compared with the dry-mixing of GNPs and these composites. The optimal piezoelectric performance was achieved when 0.3% GNPs were wet-mixed with a superplasticizer and a PZT/cement composite ($\varepsilon_r = 615$, $d_{33} = 123$ pC/N, and $k_t = 20.2\%$). Because the addition of GNPs considerably increased k_t, the GNP-containing cementitious composites exhibited a high efficiency of conversion between mechanical energy and electrical energy. These composites have the potential to be used as green energy materials in engineering applications.

CRediT authorship contribution statement

The corresponding author is responsible for ensuring that the descriptions are accurate and agreed by all authors.

Declaration of Competing Interest

The authors declare that they have no known competing financial interests or personal relationships that could have appeared to influence the work reported in this paper.

Data Availability

Data will be made available on request.

Acknowledgments

This work was supported by the Ministry of Science and Technology of Taiwan under grand No. MOST 105-2221-E-151-006 and MOST 108-2221-E-992-008-MY3.

References

[1] M.O. Kim, X. Qian, M.K. Lee, W.S. Park, Determination of structural lightweight concrete mix proportion for floating concrete structures, J. Kor. Soc. Coast. Ocean Eng. 29 (2017) 315–325.
[2] D. Jiang, K.H. Tan, C.M. Wang, K.C.G. Ong, H. Bra, J. Jin, M.O. Kim, Analysis and design of floating prestressed concrete structures in shallow waters, Mar. Struct. 59 (2018) 301–320.
[3] L. Lu, O. Dong, Properties of cement mortar and ultra-high strength concrete incorporating graphene oxide nanosheets, Nanomaterials 7 (2017) 187.
[4] L. Yu, R. Wu, Using graphene oxide to improve the properties of ultra-high-performance concrete with fine recycled aggregate, Constr. Build. Mater. 259 (2020), 120657.
[5] Y.Y. Wu, J. Zhang, C. Liu, Z. Zheng, P. Lambert, Effect of graphene oxide nanosheets on physical properties of ultra-high-performance concrete with high volume supplementary cementitious materials, Materials 13 (2020) 1929.
[6] F. Azhari, N. Banthia, Cement-based sensors with carbon fibers and carbon nanotubes for piezoresistive sensing, Cem. Concr. Comp. 34 (7) (2012) 866–873.
[7] W. Dong, W. Li, Z. Tao, K. Wang, Piezoresistive properties of cement-based sensors: Review and perspective, Constr. Build. Mater. 203 (2019) 146–163.
[8] A.Y. Jang, S.H. Lim, D.H. Kim, H.D. Yunb, G.C. Lee, S.Y. Seo, Strain-detecting properties of hybrid PE and steel fibers reinforced cement composite (Hy-FRCC) with multi-walled carbon nanotube (MWCNT) under repeated compression, Results Phys. 18 (2020), 103199.
[9] D.D.L. Chung, Self-sensing concrete: from resistance-based sensing to capacitance-based sensing, Int. J. Smart Nano Mater. 12 (2021) 1–19.
[10] M. Seifan, A.K. Samani, A. Berenjian, Bioconcrete: next generation of self-healing concrete, Appl. Microbiol. Biotechnol. 100 (2016) 2591–2602.
[11] K. Vijay, M. Murmu, S.V. Deo, Bacteria based self healing concrete – A review, Constr. Build. Mater. 152 (2017) 1008–1014.
[12] A. Al-Tabbaa, C. Litina, P. Giannaros, A. Kanellopoulos, L. Souza, First UK field application and performance of microcapsule-based self-healing concrete, Constr. Build. Mater. 208 (2019) 669–685.
[13] Z.J. Li, D. Zhang, K. Wu, Cement-based 0-3 piezoelectric composites, J. Am. Ceram. Soc. 85 (2002) 305–313.
[14] A. Chaipanich, R. Rianyoi, R. Potong, N. Jaitanong, Aging of 0–3 piezoelectric PZT ceramic–Portland cement composites, Ceram. Int. 40 (2014) 13579–13584.
[15] H.H. Pan, D.-H. Lin, R.-H. Yang, High Piezoelectric and dielectric properties of 0–3 PZT/cement composites by temperature treatment, Cem. Conc. Compos. 72 (2016) 1–8.
[16] H.H. Pan, M.W. Huang, Piezoelectric cement sensor-based electromechanical impedance technique for the strength monitoring of cement mortar, Constr. Build. Mater. 254 (2020), 119307.
[17] S. Chuah, Z. Pan, J.G. Sanjayan, C.M. Wang, W.H. Duan, Nano reinforced cement and concrete composites and new perspective from graphene oxide, Constr. Build. Mater. 73 (2014) 113–124.
[18] M. Saafi, L. Tang, J. Fung, M. Rahman, J. Liggat, Enhanced properties of graphene/fly ash geopolymeric composite cement, Cem. Concr. Res. 67 (2015) 292–299.
[19] Z. Pan, L. He, L. Qiu, A.H. Korayem, G. Li, J.W. Zhu, F. Collins, D. Li, W.H. Duan, M.C. Wang, Mechanical properties and microstructure of a graphene oxide-cement composite, Cem. Concr. Comp. 58 (2015) 140–147.
[20] H. Yang, M. Monasterio, H. Cui, N. Han, Experimental study of the effects of graphene oxide on microstructure and properties of cement paste composite, Compos. Part A 102 (2017) 263–272.
[21] S. Bai, L. Jiang, N. Xu, M. Jin, S. Jiang, Enhancement of mechanical and electrical properties of graphene/cement composite due to improve dispersion of graphene by addition of silica fume, Constr. Build. Mater. 164 (2018) 433–441.
[22] J. Liu, J. Fu, T. Ni, Y. Yang, Fracture toughness improvement of multi-wall carbon nanotubes/graphene sheets reinforced cement paste, Constr. Build. Mater. 200 (2019) 530–538.
[23] H. Peng, Y. Ge, C.S. Cai, Y. Zhang, Z. Liu, Mechanical properties and microstructure of graphene oxide cement-based composites, Constr. Build. Mater. 194 (2019) 102–109.
[24] Y.Y. Wu, L. Que, Z. Cui, P. Lambert, Physical properties of concrete containing graphene oxide nanosheets, Materials 12 (2019) 1707.
[25] C. Liu, X. Huang, Y.Y. Wu, X. Deng, J. Liu, Z. Zheng, D. Hui, Review on the research progress of cement-based and geopolymer materials modified by graphene and graphene oxide, Nanotechnol. Rev. 9 (2020) 155–169.
[26] S.C. Devi, R.A. Khanb, Effect of graphene oxide on mechanical and durability performance of concrete, J. Build. Eng. 27 (2020), 101007.
[27] W. Liang, G. Zhang, Effect of reduced graphene oxide on the early-age mechanical properties of geopolymer cement, Mater. Lett. 276 (2020), 128223.

[28] K. Chintalapudi, R.M.R. Pannem, Enhanced strength, microstructure, and thermal properties of Portland pozzolana fly ash-based cement composites by reinforcing graphene oxide nanosheets, J. Build. Eng. 42 (2021), 102521.
[29] C. Liu, X. Huang, Y.Y. Wu, X. Deng, Z. Zheng, The effect of graphene oxide on the mechanical properties, impermeability and corrosion resistance of cement mortar containing mineral admixtures, Constr. Build. Mater. 288 (2021), 123059.
[30] Q. Zheng, B. Han, X. Cui, X. Yu, J. Ou, Graphene-engineered cementitious composites: small makes a big impact, Nanomater. Nanotechnol. 7 (2017) 1–18.
[31] Q. Wang, X. Cui, J. Wang, S. Li, C. Lv, Y. Dong, Effect of fly ash on rheological properties of graphene oxide cement paste, Constr. Build. Mater. 138 (2017) 35–44.
[32] Q. Liu, Q. Xu, Q. Yu, R. Gao, T. Tong, Experimental investigation on mechanical and piezoresistive properties of cementitious materials containing graphene and graphene oxide, Constr. Build. Mater. 127 (2016) 565–576.
[33] Q. Li, C. He, H. Zhou, Z. Xie, D. Li, Effects of polycarboxylate superplasticizer-modified graphene oxide on hydration characteristics and mechanical behavior of cement, Constr. Build. Mater. 272 (2021), 121904.
[34] Q. Wang, G. Qi, D. Zhan, Y. Wang, H. Zheng, Influence of the molecular structure of a polycarboxylate superplasticizer on the dispersion of graphene oxide in cement pore solutions and cement-based composites, Constr. Build. Mater. 272 (2021), 121969.
[35] J. Liu, J. Fu, Y. Yang, C. Gu, Study on dispersion, mechanical and microstructure properties of cement paste incorporating graphene sheets, Constr. Build. Mater. 199 (2019) 1–11.
[36] M. Cayambe, C. Zambrano, T. Tene, M. Guevara, G. Tubon Usca, H. Brito, R. Molina, D. Coello-Fiallos, L.S. Caputi, C. Vacacela Gomez, Dispersion of graphene in ethanol by sonication, Mater. Today Proc. 37 (2021) 4027–4030.
[37] M. Sandhya, D. Ramasamy, K. Sudhakar, K. Kadirgama, W.S.W. Harun, Ultrasonication an intensifying tool for preparation of stable nanofluids and study the time influence on distinct properties of graphene nanofluids– a systematic overview, Ultrason. Sonochem. 73 (2021), 105479.
[38] R. Guo, Y. Suo, H. Xia, Y. Yang, Q. Ma, F. Yan, Study of piezoresistive behavior of smart cement filled with graphene oxide, Nanomater 11 (2021) 206.
[39] Q. Li, Y. Liu, D. Chen, J. Miao, S. Lin, D. Cui, Highly sensitive and flexible piezoresistive pressure sensors based on 3D reduced graphene oxide aerogel, IEEE Elect. Dev. Lett. 42 (2021) 589–592.
[40] M. Saafi, L. Tang, J. Fung, M. Rahman, F. Sillars, J. Liggat, X. Zhou, Graphene/fly ash geopolymeric composites as self-sensing structural materials, Smart Mater. Struct. 23 (2014), 065006.
[41] L. Verdolotti, C. Santillo, G. Rollo, G. Romanelli, M. Lavorgna, B. Liguori, G. C. Lama, E. Preziosi, R. Senesi, C. Andrean, M. di Prisco, MWCNT/rGO/natural rubber latex dispersions for innovative, piezo-resistive and cement-based composite sensors, Sci. Repo 11 (2021) 18975.
[42] J. Tao, X. Wang, Z. Wang, Q. Zeng, Graphene nanoplatelets as an effective additive to tune the microstructures and piezoresistive properties of cement-based composites, Constr. Build. Mater. 209 (2019) 665–678.
[43] S. Wang, A. Singh, Q. Liu, Experimental study on the piezoresistivity of concrete containing steel fibers, carbon black and graphene, Front. Mater. 8 (2021), 652614.
[44] Z. Ge, J. Qin, R. Sun, Y. Guan, H. Zhang, Z. Wang, The effect of the addition of graphene nanoplatelets on the selected properties of cementitious composites, Front. Built Environ. 7 (2021), 673346.
[45] H. Liu, A. Deshmukh, N. Salowitz, J. Zhao, K. Sobolev, Resistivity Signature of graphene-based fiber-reinforced composites subjected to mechanical loading, Front. Mater. 9 (2022), 818176.
[46] W. Dong, W. Li, Y. Guo, K. Wang, D. Sheng, Mechanical properties and piezoresistive performances of intrinsic graphene nanoplate/cement-based sensors subjected to impact load, Constr. Build. Mater. 327 (2022), 126978.
[47] D. Xu, S. Huang, X. Cheng, Electromechanical impedance spectra investigation of impedance-based PZT and cement/polymer based piezoelectric composite sensors, Constr. Build. Mater. 65 (2014) 543–550.
[48] J. Zhang, Y. Lu, Z. Lu, C. Liu, G. Sun, Z. Li, A new smart traffic monitoring method using embedded cement-based piezoelectric sensors, Smart Mater. Struct. 24 (2015), 025023.
[49] H.H. Pan, J.C. Guan, Stress and strain behavior monitoring of concrete through electromechanical impedance using piezoelectric cement sensor and PZT sensor, Constr. Build. Mater. 324 (2022), 126685.
[50] Z.J. Li, D. Zhang, K.R. Wu, Cement matrix 2–2 piezoelectric composite–Part 1 sensory effect, Mater. Struct. 34 (2001) 506–512.
[51] K.H. Lam, H.L.W. Chan, Piezoelectric cement-based 1–3 composites, Appl. Phys. A 81 (2005) 1451–1454.
[52] Z.J. Li, B. Dong, D. Zhang, Influence of polarization on properties of 0–3 cement-based PZT composites, Cem. Concr. Compos. 27 (2005) 27–32.
[53] S. Huang, J. Chang, L. Lu, F. Liu, Z. Ye, X. Cheng, Preparation and polarization of 0–3 cement based piezoelectric composites, Mater. Res. Bull. 41 (2006) 291–297.
[54] B. Dong, F. Xing, Z. Li, The study of poling behavior and modeling of cement-based piezoelectric ceramic composites, Mater. Sci. Eng. A 456 (2007) 317–322.
[55] A. Chaipanich, N. Jaitanong, Effect of poling time on piezoelectric properties of 0–3 PZT-portland cement composites, Ferroelectr. Lett. 35 (2008) 73–78.
[56] H.H. Pan, C.K. Wang, Y.C. Cheng, Curing time and heating conditions for piezoelectric properties of cement-based composites containing PZT, Constr. Build. Mater. 129 (2016) 140–147.
[57] H.H. Pan, C.K. Wang, M. Tia, Y.M. Su, Influence of water-to-cement ratio on piezoelectric properties of cement-based composites containing PZT particles, Constr. Build. Mater. 239 (2020), 117858.
[58] A. Chaipanich, Dielectric and piezoelectric properties of PZT–silica fume cement composites, Curr. Appl. Phys. 7 (2007) 532–536.
[59] F. Wang, H. Wang, Y. Song, H. Sun, High piezoelectricity 0–3 cement-based piezoelectric composites, Mater. Lett. 76 (2012) 208–210.
[60] H.H. Pan, D.H. Lin, R.H. Yeh, Influence of pozzolanic materials on 0–3 cement-based piezoelectric composites, in: Yazdani, S., Singh, A. (Eds), New Development Structure Engineering & Construction (2013) 929–934.
[61] N. Jaitanong, K. Wongjinda, P. Tammakun, G. Rujijanagul, A. Chaipanich, Effect of carbon addition on dielectric properties of 0–3 PZT-Portland cement composite, Adv. Mater. Res. 55–57 (2008) 377–380.
[62] H. Gong, Z.J. Li, Y. Zhang, R. Fan, Piezoelectric and dielectric behavior of 0–3 cement-based composites mixed with carbon black, J. Eur. Ceram. Soc. 29 (2009) 2013–2019.
[63] S. Huang, X. Li, F. Liu, L. Chang, D. Xu, X. Cheng, Effect of carbon black on properties of 0–3 piezoelectric ceramic/cement composites, Curr. Appl. Phys. 9 (2009) 1191–1194.
[64] H.H. Pan, W.R. Lin, K. Huang, Piezoelectric properties of cement piezoelectric composites containing nano-quartz powders, in: H. Askarinejad, Yazdani, S., Singh, A. (Eds), Proc. Inter. Struct. Eng. Constr. 7(2), 2020, SUS-02.
[65] H. Gong, Y. Zhang, J. Quan, S. Che, Preparation and properties of cement based piezoelectric composites modified by CNTs, Curr. Appl. Phys. 11 (2011) 653–656.
[66] H.H. Pan, R.H. Yang, T.C. Cheng, High piezoelectric properties of cement piezoelectric composites containing kaolin, Proc. SPIE 943 (2015) 94370R.
[67] Z. Chang, W. Yan, J. Shang, J.Z. Liu, Piezoelectric properties of graphene oxide: a first-principles computational study, Appl. Phys. Lett. 105 (2014), 023103.
[68] S. Candamano, E. Sgambitterra, C. Lamuta, L. Pagnotta, S. Chakraborty, F. Crea, Graphene nanoplatelets in geopolymeric systems: a new dimension of nanocomposites, Mater. Lett. 236 (2019) 550–553.
[69] N.S. Danial, D.S. Che Halin, M.M. Ramli, M.M.A. Abdullah, M.A.A. Salleh, S.S. Mat Isa, L.F. Talip, N.S. Mazlan, Graphene geopolymer hybrid: a review on mechanical properties and piezoelectric effect, IOP Conf. Ser. Mater. Sci. Eng. 572 (2019), 012038.
[70] N. Jaitanong, S. Narksitipan, A. Ngamjarurojana, A. Chaipanich, Influence of graphene nanoplatelets on morphological and electric properties of silica fume blended cement–piezoelectric ceramic composite, Ceram. Int. 44 (2018) S137–S140.
[71] E. Shamsaei, F.B. de Souza, X. Yao, E. Benhelal, A. Akbari, W. Duan, Graphene-based nanosheets for stronger and more durable concrete: a review, Constr. Build. Mater. 183 (2018) 642–660.
[72] A.M. Sabziparvar, E. Hosseini, V. Chiniforush, A.H. Korayem, Barriers to achieving highly dispersed graphene oxide in cementitious composites: an experimental and computational study, Constr. Build. Mater. 199 (2019) 269–278.
[73] J.I. Roscow, C.R. Bowen, D.P. Almond, Breakdown in the case for materials with giant permittivity? ACS Energy Lett. 2 (2017) 2264–2269.
[74] X. Cheng, S. Huang, J. Chang, R. Xu, F. Liu, L. Lu, Piezoelectric and dielectric properties of piezoelectric ceramic–sulphoaluminate cement composites, J. Eur. Ceram. Soc. 25 (2005) 3223–3228.
[75] APC International Ltd, Piezoelectric ceramics: Principles and applications, published by APC International Ltd., Mackeyville, Pennsylvania, USA, 2002.
[76] H.H. Pan, C.K. Chiang, Effect of aged binder on piezoelectric properties of cement-based piezoelectric composites, Acta Mech. 225 (2014) 1287–1299.

Huang Hsing Pan: A professor works in the Department of Civil Engineering at the National Kaohsiung University of Science and Technology (NKUST) located in Kaohsiung, Taiwan, since August 1992. He received his Ph.D. degree from the Department of Mechanical and Aerospace Engineering at the Rutgers University, New Brunswick, New Jersey, United States in June, 1992. He has been serving as a board of director of Taiwan Concrete Institute (TCI). His research interests cover: cement-based piezoelectric composites, micromechanics of cement-matrix composites, structural health monitoring, and smart technologies.